

Evaluation of the three different wind components

This supplement evaluates the three wind components of COSMO_{iso}. First, the horizontal wind components are addressed. Second, the mesoscale vertical velocity at cloud base is discussed.

The numerical simulations, ECHAM6-wiso, COSMO_{iso,10km}, COSMO_{iso,5km}, and COSMO_{iso,1km}, as well as the data from the HALO dropsondes (George et al., 2021) agree reasonably with the horizontal winds from ERA5 (taken as the reference, because the horizontal winds above 850 hPa of the numerical simulations are nudged towards ERA5; Fig.S2.1). In the layer 1000-850 hPa, the agreement is better for the zonal wind component than for the meridional wind component (TableS2.1). In the layers 1000-850 hPa and 850-300 hPa the root mean square differences relative to ERA5 are larger for the three COSMO_{iso} simulations than for ECHAM6-wiso, but are of comparable magnitude as for HALO (TableS2.1). Based on this comparison, we conclude that the horizontal winds of COSMO_{iso} have no significant biases.

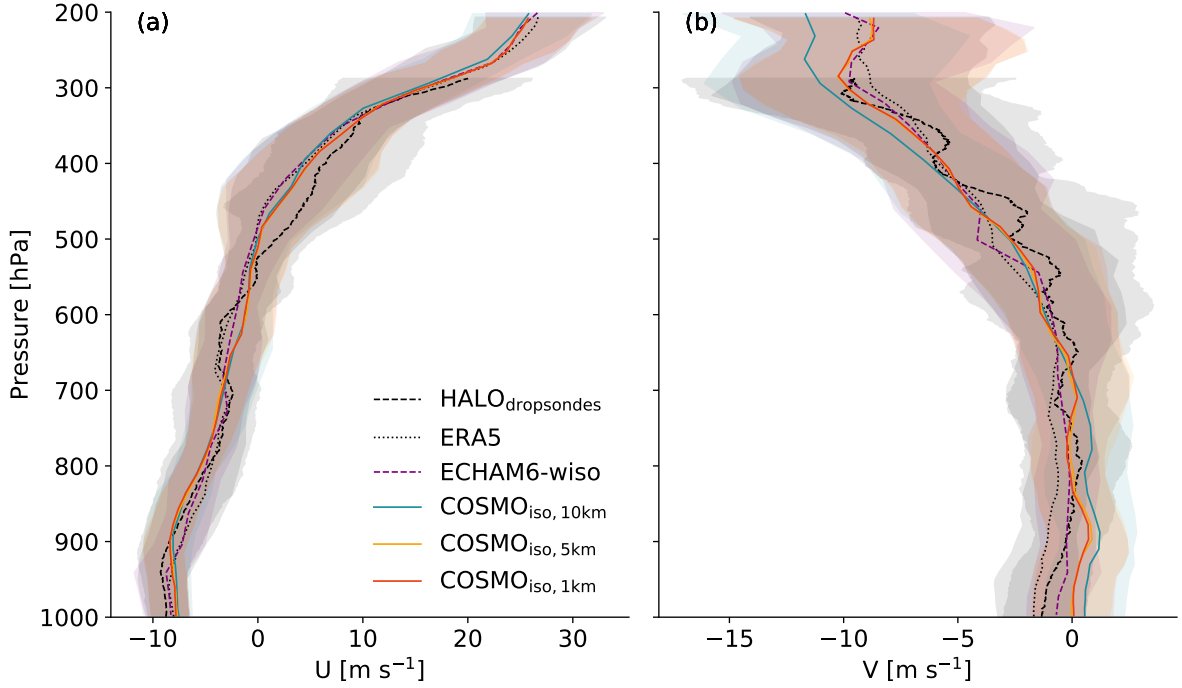


Figure S2.1: Vertical profiles of (a) the zonal wind component and (b) the meridional wind component. Shown are the median (line) and the 25-75-percentile range (shading) of the HALO dropsondes (black dashed; 810 dropsondes) and the vertical profiles closest to the centre of the EUREC⁴A circle (at 57.717° W, 13.3° N) extracted every time step from 20 January to 13 February 2020 from ERA5 (black dotted; 600 profiles), COSMO_{iso,10km} (teal; 600 profiles), COSMO_{iso,5km} (yellow; 600 profiles), COSMO_{iso,1km} (red; 600 profiles).

For the comparison of the mesoscale vertical velocity at cloud base, we first identify cloud base in the ERA5 and ECHAM6-wiso data (Fig. S2.2). For this, we repeat the procedure as described in the paper for the COSMO_{iso} simulations. The cloud base level identified in the ERA5 data alternates between five levels (model levels 77-82), which correspond roughly to 1135, 1025, 925, 830, 740, 660 m. In the ECHAM6-wiso data, only two levels (model levels 90-91), which correspond to roughly 1000 and 650 m, are identified as cloud base (Fig. S2.2). The variability of the identified cloud base levels reflects the vertical resolution of the datasets. ERA5 has more vertical levels in the lower troposphere (i.e., pressure > 850 hPa) than the COSMO_{iso} simulations and, therefore, shows a larger variability of the cloud base height. ECHAM6-wiso has fewer vertical levels in the lower troposphere than the COSMO_{iso} simulations and, therefore, shows a smaller variability of the cloud base height.

Table S2.1: Root mean square differences of the median profiles (shown in Fig.S2.1) of the HALO dropsondes, ERA5, ECHAM6-wiso, COSMO_{iso,10km}, COSMO_{iso,5km}, and COSMO_{iso,1km} data relative to the ones from the ERA5 data over the layer 1000-850 hPa (and in brackets over the layer 850-300 hPa).

| Dataset | U [m s ⁻¹] | V [m s ⁻¹] |
|---------------------------|--------------------------|--------------------------|
| HALO | 0.9 (1.5) | 0.7 (1.0) |
| ECHAM6-wiso | 0.3 (0.4) | 1.0 (0.4) |
| COSMO _{iso,10km} | 0.9 (0.9) | 2.2 (1.1) |
| COSMO _{iso,5km} | 0.9 (1.0) | 1.7 (0.7) |
| COSMO _{iso,1km} | 1.0 (1.0) | 1.7 (0.7) |

In addition, Fig.S2.2 displays the height of the subcloud-layer top h (i.e., cloud base) derived from the HALO dropsonde measurements (Vogel et al. 2022, Albright et al. 2022). The level h is defined as the height at which the virtual potential temperature (θ_v) first exceeds its density-weighted mean from 100 m up to h by a fixed threshold $\varepsilon = 0.2$ K. Cloud base altitudes identified in the COSMO_{iso}, ECHAM6-wiso, and ERA5 data tend to be higher than the observation-based (ATR and HALO) altitudes, especially in the first half of the observation period (i.e., January 2020). Nevertheless, we find several time steps (e.g., the flights on 5 or 7 February) where all datasets match well.

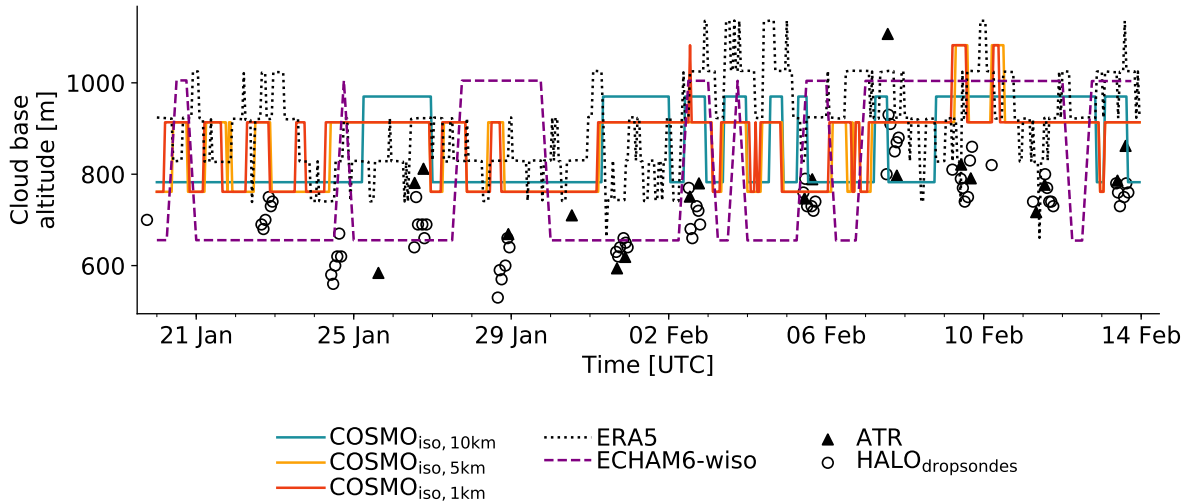


Figure S2.2: Time series of cloud base (flight) altitude. Shown are the values of the grid points in the domain 54.5-61° W, 11-16° N at every time step for ERA5 (dotted black), ECHAM6-wiso (dashed purple), COSMO_{iso,10km} (teal), COSMO_{iso,5km} (yellow), COSMO_{iso,1km} (red), and the median value (black triangles) of each ATR flight. The number of grid points in the considered domain is 35 for ECHAM6-wiso, 154 for ERA5, 3221 for COSMO_{iso,10km}, 12632 for COSMO_{iso,5km}, and 316028 for COSMO_{iso,1km}. The heights of the subcloud-layer top h derived from HALO dropsonde measurements (see the text for details) are shown as empty black circles.

For the three COSMO_{iso} simulations and the ERA5 data, we use the hourly mean vertical velocity of the cloud base grid points inside the EUREC⁴A circle as an estimate for the mesoscale vertical velocity at cloud base. The resulting values are very similar for the three COSMO_{iso} simulations (Fig.S2.3). However, the correlation between the values from ERA5 and the three COSMO_{iso} simulations remains low with values of 0.18 and 0.21, suggesting that the nudging of the horizontal winds has little influence on the vertical wind field. Although the temporal evolution of the COSMO_{iso} and the ERA5 mesoscale vertical velocities differ, the different datasets yield values in the same order of magnitude.

Another reference dataset is provided by the mesoscale vertical velocity estimates from the HALO dropsonde EUREC⁴A circle products (George et al., 2021). Vogel et al. (2022) extracted the mesoscale

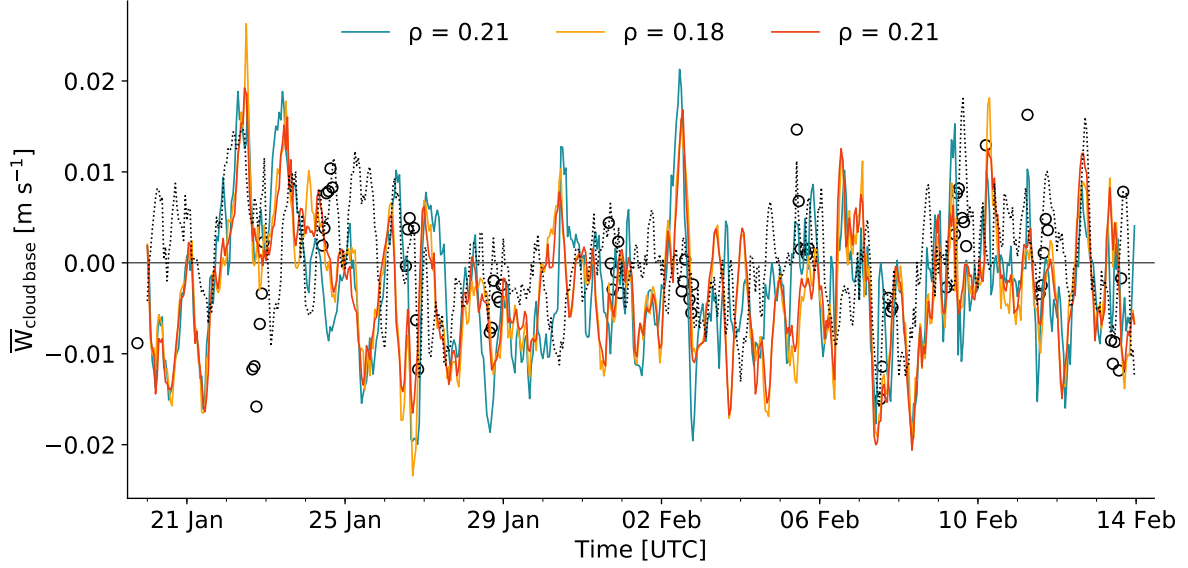


Figure S2.3: Time series of vertical velocity at cloud base. Shown are hourly mean values over the cloud base grid points inside a geographical box, which embraces the EUREC⁴A circle (56.717–58.717° W, 12.3–14.3° N). In this box, for ERA5 and the three COSMO_{iso} simulations. There are 16 grid points for ERA5, 399 for COSMO_{iso,10km} (teal), 1561 for COSMO_{iso,5km} (yellow), and 38910 for COSMO_{iso,1km} (red). The Pearson correlation coefficients (ρ) between the shown time series of ERA5 and the three COSMO_{iso} simulations (indicated by the colour) are provided. Note that there was no vertical wind component available for ECHAM6-wiso. The HALO dropsonde-based estimates of the mesoscale vertical velocity at the subcloud-layer top height (see the text for details) are shown as empty black circles.

vertical velocity at the subcloud layer top height h (Fig. S2.2) that are valid for hourly time steps. These values are shown in Fig. S2.3. For the most part, the HALO-based estimates agree well with the ERA5 data (see also George et al. 2022). The agreement between the HALO-based estimates and the three COSMO_{iso} simulations is less good as shown by the root mean square differences (Table S2.2), but still in the same order of magnitude.

Table S2.2: Root mean square differences mesoscale vertical velocities at cloud base (shown in Fig. S2.3) of ERA5, COSMO_{iso,10km}, COSMO_{iso,5km}, and COSMO_{iso,1km} data relative to the ones based on the HALO dropsonde-circle product. For ERA5, COSMO_{iso,10km}, COSMO_{iso,5km}, and COSMO_{iso,1km} the values temporally closest to the HALO time steps within the period 20 January to 13 February 2020 are taken into account (i.e., 68 data points).

| Dataset | W [m s ⁻¹] |
|---------------------------|--------------------------|
| ERA5 | 6.5×10^{-3} |
| COSMO _{iso,10km} | 10.3×10^{-3} |
| COSMO _{iso,5km} | 9.7×10^{-3} |
| COSMO _{iso,1km} | 9.2×10^{-3} |

References

- Albright, A. L., Bony, S., Stevens, B., and Vogel, R. (2022). Observed subcloud layer moisture and heat budgets in the trades. *J. Atmos. Sci.*, 79(9), 2363–2385. <https://doi.org/10.1175/JAS-D-21-0337.1>
- George, G., Stevens, B., Bony, S., Pincus, R., Fairall, C., Schulz, H., Kölling, T., Kalen, Q. T., Klingebiel, M., Konow, H., Lundry, A., Prange, M., and Radtke, J. (2021). JOANNE: Joint dropsonde Observations of the Atmosphere in tropical North atlaNtic meso-scale Environments. *Earth Syst. Sci. Data*, 13(11), 5253–5272. <https://doi.org/10.5194/essd-13-5253-2021>
- George, G., Stevens, B., Bony, S., Vogel, R., and Naumann, A. K. (2022). Ubiquity of shallow mesoscale

circulations in the trades and their influence on moisture variance. Nat. Geosci. [Preprint]. <https://doi.org/10.1002/essoar.10512427.1>

Vogel, R., Albright, A. L., Vial, J., George, G., Stevens, B., and Bony, S. (2022). Strong cloud-circulation coupling explains weak trade cumulus feedback. Nature, 612, 696–700. <https://doi.org/10.1038/s41586-022-05364-y>

Acknowledgements

We thank Raphaëla Vogel (University of Hamburg) for the provision of the subcloud-layer top (h) and mesoscale vertical velocity (W) estimates retrieved from the HALO dropsondes.